

Preparation of composite with silica-coated nanoparticles of iron oxide spinels for applications based on magnetically induced hyperthermia

Angela L. Andrade · José D. Fabris ·
Márcio C. Pereira · Rosana Z. Domingues ·
José D. Ardisson

Published online: 1 November 2012
© Springer Science+Business Media Dordrecht 2012

Abstract It is reported a novel method to prepare magnetic core (iron oxide spinels)–shell (silica) composites containing well-dispersed magnetic nanoparticles in aqueous solution. The synthetic process consists of two steps. In a first step, iron oxide nanoparticles obtained through co-precipitation are dispersed in an aqueous solution containing tetramethylammonium hydroxide; in a second step, particles of this sample are coated with silica, through hydrolyzation of tetraethyl orthosilicate. The intrinsic atomic structure and essential properties of the core–shell system were assessed with powder X-ray diffraction, Fourier transform infrared spectrometry, Mössbauer spectroscopy and transmission electron microscopy. The heat released by this ferrofluid under an AC-generated magnetic field was evaluated by following

A. L. Andrade
Department of Chemistry, Federal University of Ouro Preto (UFOP),
35400-000 Ouro Preto, Minas Gerais, Brazil

J. D. Fabris (✉)
Federal University of Jequitinhonha and Mucuri Valleys (UFVJM),
39100-000 Diamantina, Minas Gerais, Brazil
e-mail: jdfabris@ufmg.br

M. C. Pereira
Institute of Science, Engineering and Technology,
Federal University of Jequitinhonha and Mucuri Valleys (UFVJM),
39803-371 Teófilo Otoni, Minas Gerais, Brazil

R. Z. Domingues
Department of Chemistry, Federal University of Minas Gerais (UFMG),
31270-901 Belo Horizonte, Minas Gerais, Brazil

J. D. Ardisson
Laboratory of Applied Physics,
Development Center of Nuclear Technology (CNEN/CDTN),
31270-901 Belo Horizonte, Minas Gerais, Brazil

the temperature evolution under increasing magnetic field strengths. Results strongly indicate that this ferrofluid based on silica-coated iron oxide spinels is technologically a very promising material to be used in medical practices, in oncology.

Keywords Biomedicine · Nanotechnology · Magnetic hyperthermia · Ferrofluid

1 Introduction

Different chemical methods have been used or reportedly proposed to synthesize and prepare magnetic nanoparticles (MNPs) of iron oxide spinels, namely maghemite ($\gamma\text{-Fe}_2\text{O}_3$) and magnetite (Fe_3O_4), with variable mean sizes and homogeneous morphology, for technological applications in clinical diagnostics and medical therapies [1–6]. This increasing interest in designing and developing MNPs is due to their unique physical and chemical properties for such purposes. In particular, to their magnetic anisotropy, which can be pronouncedly higher than those of the corresponding bulk specimen.

With proper surface coating, those MNPs can be dispersed into selected solvents to form homogeneous suspensions, known as ferrofluids [7, 8]. The surfaces of particles may be suitably modified with an organic polymer, a metallic (e.g. gold) or an oxide (e.g. silica or alumina) layer to make them suitably functional, as by further coating with various bioactive molecules [9]. Such suspensions can be driven, under the action of an externally applied magnetic field, to be concentrated in selected internal parts of the living body, enabling them to be used in medical therapies that demand local tissue heating or delivering of bioactive molecules [10]. For such applications, the particle must combine high magnetic saturation, biocompatibility and interactive functions at its surface.

Biomedical applications of ferrofluids include magnetic separation, drug delivery, magnetic resonance imaging (MRI), and hyperthermia [11–14]. Hyperthermia means that the magnetic nanosystems can heat up under the action of a magnetic field, releasing thermal energy that may be dimensioned to directly kill tumor cells (a moderate degree of heating may result in an effective cell destruction), or to be used as a programmable local delivery of chemicals, in chemotherapy, or even of radiotherapeutic agents [15].

The use of hyperthermia (heating) to treat tissues with malignant tumors is as old as the medicine itself. Hippocrates, the Father of Medicine, proposed that the surface of tumors should be cauterized by heating them with a hot iron piece. In our modern times, more sophisticated methods (hot water bath, pyrogens such as mixed bacterial toxins, perfusion heating, high-frequency radiation, magnetic fluid hyperthermia) are used to heat, and hopefully destroy tumors [16].

Magnetically induced hyperthermia, one of the sought procedures for local therapy to treat cancers, is based on the exposition of cancerous tissues, which was made covered with a ferrofluid, to an alternating magnetic field. Ferrofluids for this purpose imply a system containing MNPs in a carrier fluid that would be directly injected to the tumor area in the body or to the blood stream, alternatively also mixed with a specific tumor antibody targeting. Once the ferrofluid is placed in the selected vital area of the living body, an alternating magnetic field is externally applied. The field strength must be dimensioned basing on the resulting hyperthermic temperature,

being limited to a value that is assured to not affect the healthy cells. Up to this limit, the magnetic field can be safely applied so to reach any deeper parts of the living body. The magnetic particles respond to the variable magnetic field by releasing heat due to magnetic hysteresis losses. Magnetic particles embedded around a tumor site and subject to an oscillating magnetic field will heat up to a temperature that depends on the magnetic properties of the material, the strength of the magnetic field, on the oscillation frequency and on the cooling capacity of the blood flow surrounding the tumor site. Cancer cells are destroyed at temperatures slightly higher than 43 °C; the normal cells can survive even at temperatures moderately above that limit. Hyperthermia in this sense is still an under development technique for local therapy in oncology. The procedure has also the advantage to prevent many side effects, so commonly observed in patients under treatment with chemotherapy or radiotherapy.

Herein, we present the preparation of a ferrofluid based on well dispersed core-shell system formed by iron oxide spinels (particle cores) coated with silica (shell) to produce magnetically induced hyperthermia. The core-shell system was prepared *via* a two-step process: firstly, iron oxide nanoparticles (sample Mt) were obtained through co-precipitation, and this material was dispersed in an aqueous solution containing tetramethylammonium hydroxide (TMAOH) (sample Mt1). In a second step, particles of the sample Mt1 were coated with silica (sample Mt1-Si2), through hydrolyzation of tetraethyl orthosilicate (TEOS). The obtained ferrofluid is intended to be a basic material for potential technological applications in medical therapies in oncology.

2 Experimental

2.1 Materials and reagents

All chemicals used in this work, namely iron (III) chloride hexahydrate, $\text{FeCl}_3 \cdot 6\text{H}_2\text{O}$ (Riedel-de Haen); hydrochloride acid, HCl (Fluka); sodium sulfide, Na_2SO_3 (Sigma, Aldrich); ammonium hydroxide, NH_4OH (Fluka); 25 % aqueous tetramethylammonium hydroxide solution, $\text{C}_4\text{H}_{13}\text{NO} \cdot 5\text{H}_2\text{O}$ (TMAOH) (Vetec); absolute ethanol, $\text{CH}_3\text{CH}_2\text{OH}$ (Panreac, 99.5 %) and tetraethyl orthosilicate, $(\text{C}_2\text{H}_5\text{O})_4\text{Si}$ (TEOS) (Aldrich, 98 %) were of analytical grade standards and used as received.

2.2 Iron oxide nanoparticles preparation

The synthesis procedure followed to prepare these iron oxide spinels samples was described in more details in ref. [2]. It was based on the method earlier proposed by Qu et al. [17]: 30 mL of a $\text{FeCl}_3 \cdot 6\text{H}_2\text{O}$ stock solution containing 2 mol L^{-1} (dissolved in 0.5 mol L^{-1} HCl), 20 mL of a Na_2SO_3 stock solution with 1 mol L^{-1} and 50.8 mL of a NH_4OH solution diluted to a total volume of 800 mL were used. Just after mixing Fe^{3+} and SO_3^{2-} , the obtained solution was kept under vacuum pressure for 1 min. Initially, the color of the solution changed from yellow to red; after few minutes, the yellow reappeared. Diluted ammonia solution was then quickly poured into the mixture under vigorous stirring, and vacuum, for 1 min. The stirring was continued for an additional 30 min, after the black precipitate was formed. The

suspension containing the precipitated was centrifuged at 2,000 rpm for 3 min; the supernatant was discarded. This procedure was repeated five times by re-dispersing the resulting cakes in distilled water. The as obtained precipitate was labeled Mt. The nanoparticles were then coated with tetramethylammonium hydroxide (TMAOH). Typically, 1 mL of commercial 25 % TMAOH solution was added to each centrifuge tube containing an amount of wet cake corresponding to about 1 g dry powder and re-dispersed with a thin glass rod until obtaining homogeneous suspensions. This sample was labeled Mt1. 1 mL of this suspension was diluted ten times in distilled water and the obtained ferrofluid was used for further coating with silica, to produce the sample Mt1-Si2, in an alkaline alcohol/water mixture at room temperature by using the ferrofluid as seed, according to the method originally proposed by Stöber [18], with some modification [19]. This Mt1-Si2 sample was prepared by adding 2 mL of diluted Mt1 suspension in 160 mL of absolute ethanol at room temperature, followed by ultrasonication for 5 min. Following that, 2 mL of TEOS and 40 mL of distilled water were added and the mixture was stirred at room temperature for 1 day long. The as coated magnetic powder was centrifuged at 16,000 rpm for 20 min, washed thrice with distilled water and acetone.

The resulting products were separated with a small hand magnet, washed out with distilled water and acetone, and dried at room temperature.

2.3 Preparation of glass used as control sample for the zeta potential measurements

A silicon-based glass was prepared the following way: TEOS was added to an acidified (HCl—pH 1.7) aqueous solution, and next added with ethanol in a molar proportion of H₂O:TEOS:CH₃CH₂OH of 4:1:4. The solution was magnetically stirred until gelling. The material was placed under a humidified atmosphere overnight, and treated next at 400 °C for 2 h. The resulting glass was used as a control sample for zeta potential measurements.

2.4 Characterization

Electron micrographs of the iron oxide spinels dispersions were carried out with a conventional transmission electron microscopy (TEM). The iron oxide spinels dispersions powder were embedded in an Epofix TM resin to form a block which was cleaved; thin slices (50 nm) were then cut with an Ultramicrotome (Leica UC6), provided with a diamond knife, and deposited onto a holey carbon coated TEM grid. This TEM grid was then dried in a vacuum desiccator. The crystalline structure of the magnetic nanoparticles, after the liquid carrier of samples was evaporated, were assessed with powder X-ray diffraction (XRD) measurements, using a Shimadzu XRD 6000 diffractometer equipped with an iron tube (40 kV and 30 mA) and a graphite monochromator. The scans were done between 15 and 70° (2 θ) with a scanning speed of 1°/min. The identification of crystalline phases was performed with the Jade + software (Materials Data, Inc.). Silicon was used as an internal standard. FTIR data were obtained with a Perkin Elmer Spectrum GX spectrophotometer. The solids were homogeneously dispersed in KBr (1 wt% approximately) and pressed into discs. Spectra were recorded with a resolution of 4 cm⁻¹ with 16 scans per spectrum. Mössbauer spectra were collected with a constant acceleration transmission mode setup, with a ~50 mCi ⁵⁷Co/Rh gamma-ray source.

Spectra at 298 K and 80 K were obtained with a spectrometer equipped with a transducer (CMTE model MA250) controlled by a linear function driving (CMTE model MR351). Values of Mössbauer isomer shifts are quoted relatively to α -Fe. The experimental reflections were fitted to Lorentzian functions by least-square fitting with software NORMOSTM-90 (developed by R. A. Brand, at Laboratorium für Angewandte Physik, Universität Duisburg, D-47048, Duisburg-Germany).

The determination of zeta potential (ζ) was performed on a Coulter Delsa 440SX, by using a stock suspension of the ground material in deionized water, prepared and homogenized by ultrasonication for 15 min. Drops of this stock suspension were then added to an aqueous solution of KCl 10^{-3} mol L⁻¹ for the zeta potential measurements. The pH of the measuring solution was varied and adjusted to several values, in the pH range of 2–8, by using 10^{-3} mol L⁻¹ aqueous solutions of KOH and HNO₃.

Heat dissipation experiments were carried out by transferring the suspensions with dispersed iron oxide spinels in both water and hydrogel into a test tube. A three-loop coil (Nova Star 5kW RF Power Supply, Ameritherm, Inc) with resonant frequency of 220 kHz and 198 kHz was used in the experiments, in order to study the correlation between the applied magnetic field and the AC magnetically induced heating temperature. The sample concentration was approximately 4 mg mL⁻¹ in water and 4 mg g⁻¹ in polyvinyl alcohol hydrogel. In the hydrogel-dispersed samples, rotation of particles was restricted and the magnetic moment relaxed only through Néel relaxation. The temperature of the magnetic suspension was measured with an optical fiber thermometer. Results were taken as the mean of triplicate measurements. The amount of heat generated by pure water and pure hydrogel in the two AC magnetic fields was measured, in an attempt to obtain any contribution of water and hydrogel to rise the temperature by dispersing nanoparticles. The whole contribution of both pure water and gel was discounted from the final temperature value for each ferrofluid.

The polyvinyl alcohol hydrogel was based on the method earlier proposed by Hyon et al. [20], with minor modifications [21]. A homogeneous PVA solution with a PVA concentration of 15 wt% was obtained by heating the mixture of PVA and a mixed water/DMSO solvent at 140 °C for 2 h. The mixing ratio of water to DMSO was kept to 20:80, by weight. Then the casted PVA was placed in a freezer at -20 °C for 24 h.

3 Results and discussion

The size and morphology of particles by comparing TEM pictures of the samples Mt and Mt1 was described in details in ref. [1]. It can be observed that the particles in Mt1 were better dispersed than in Mt. This may be explained by assuming that the tetramethylammonium hydroxide (TMAOH) acts as a surface-active agent [22] favoring the dispersion of iron oxide nanoparticles. Figure 1 shows typical TEM images of the Mt1-Si2 sample. It was observed that the core particles are spherical in shape and is covered with a uniform and continuous dense layer on a surface containing multi-cores of iron oxide nanoparticles. Because the atomic number for iron is higher than that for silicon, the TEM micrographs show cores in darker than shells.

Fig. 1 TEM micrograph of sample Mt1-Si2

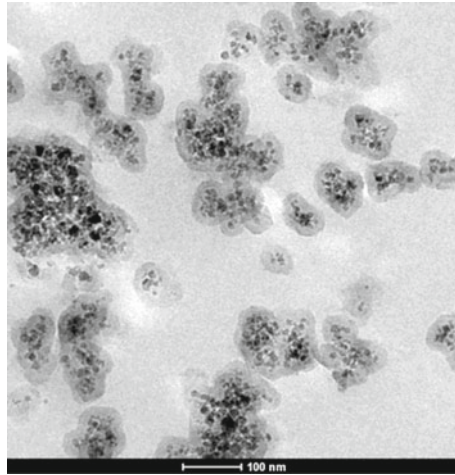


Fig. 2 ATR-FTIR spectra for TMA-OH, Mt, Mt-1, and Mt1-Si2

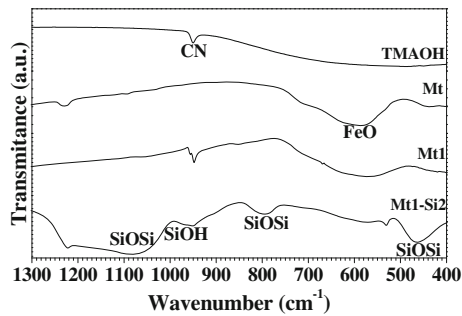


Figure 2 depicts the FTIR spectra of the tetramethylammonium hydroxide (TMAOH), iron oxide spinels (Mt), TMAOH coated iron oxide spinels (Mt1), and silica coated Mt1 (Mt1-Si2) samples. The spectrum for sample TMAOH shows a strong band at 950 cm^{-1} , assignable to the asymmetric methyl deformation mode C–N, which is generally observed in the domain $900\text{--}1000\text{ cm}^{-1}$ [23]. Consistently, this same band at 950 cm^{-1} is observed for sample Mt1-Si2, originated from the TMAOH itself or to Si–OH, resulting from the incomplete condensation of TEOS [24]. The absorption peak of iron oxide spinels of Fe–O bond at around 570 cm^{-1} [25–27] is clearly visible in the spectrum for samples Mt, Mt1 and Mt1-Si2. Comparably, one new absorption peak for samples Mt1 and Mt1-Si2 that appears at 950 cm^{-1} is due to the transmittance bands typical of TMAOH. Furthermore, two absorption peaks centered at around 805 and 1093 cm^{-1} can also be observed for Mt1-Si2 sample, corresponding to the stretching of Si–O–Si bond from the silica particles. From the above results, it can be inferred that the TMAOH and SiO_2 have been successfully coated on the surface of iron oxide nanoparticles and that the sample Mt does not change chemically or physically after the treatment with TMAOH and TEOS.

Mössbauer spectra at 298 K for all the samples (Fig. 3a; hyperfine parameters, Table 1) exhibited rather complex spectral patterns, with broad and asymmetric resonance lines due to distribution of particle size and different degrees of oxidation

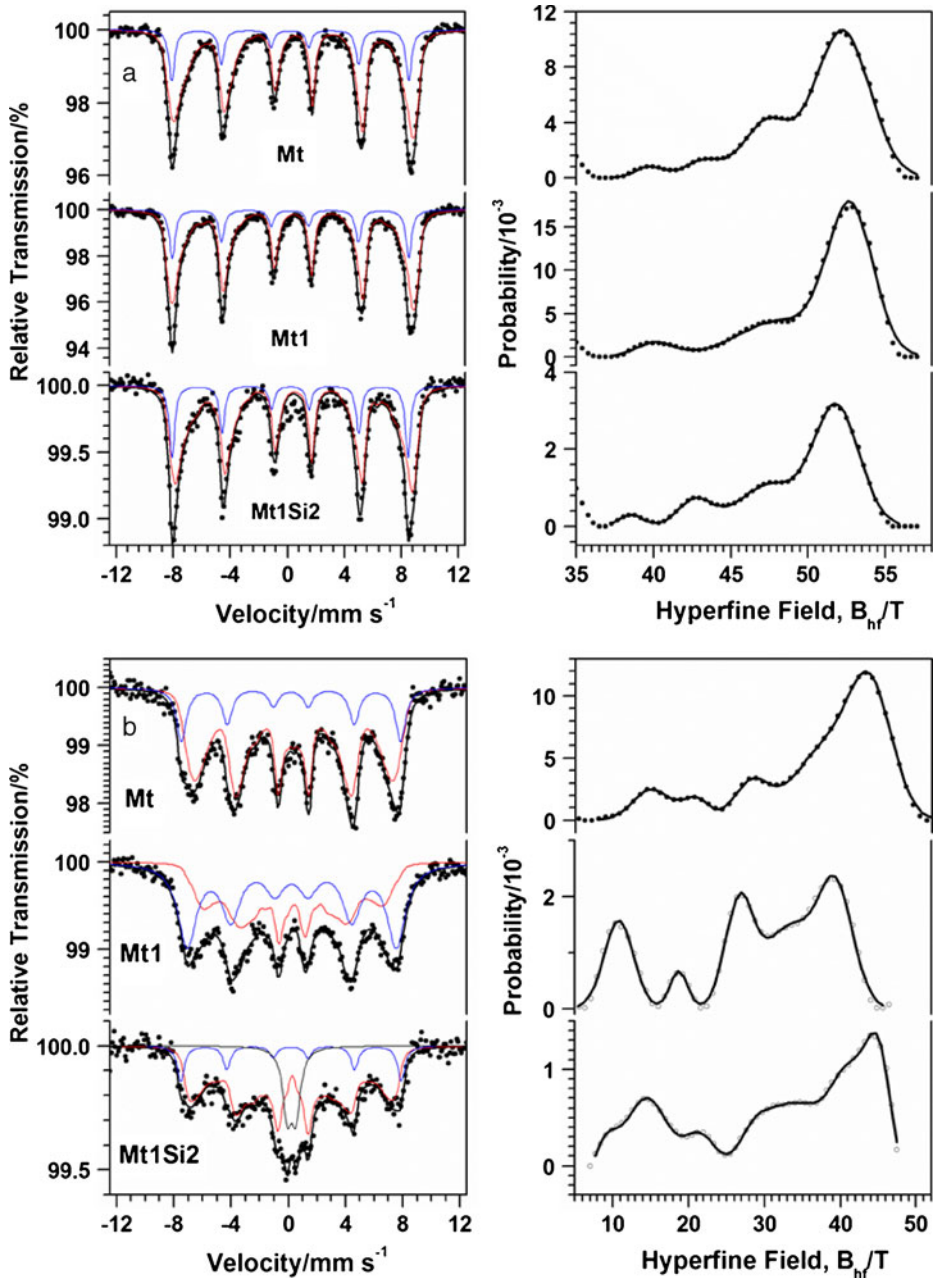


Fig. 3 Mössbauer spectra and corresponding probability profiles of hyperfine field values for samples Mt, Mt1, and Mt1Si2 at: **a** 80 K and **b** 298 K

of Fe^{2+} in the iron oxide spinels. A typical spectrum for magnetite is characterized by two subspectra: one due to Fe^{3+} in tetrahedral coordination site and other to the mixed valence $\text{Fe}^{3+}/\text{Fe}^{2+}$ in octahedral sites. From the spectrum for the sample

Table 1 Hyperfine parameters of the fitted Mössbauer spectra recorded at 298 K

Sample	$\delta/\text{mm s}^{-1}$	$\varepsilon, \Delta/\text{mm s}^{-1}$	B_{hf}/T	RA/%
Mt	0.29	0.02	47.5	20
	0.48	0.01	43.9 ^a	80
Mt1	0.34	0.03	45.3	51
	0.42	0.05	39.5 ^a	49 [#]
Mt1Si2	0.34	0.03	47.8	12
	0.40	-0.06	45.1 ^a	74
	0.37	0.60	—	13

δ = isomer shift relative to αFe ; ε = quadrupole shift; Δ = quadrupole splitting; B_{hf} = hyperfine field and RA = relative subspectral area

^aHyperfine field at maximum probability of the hyperfine field distribution profile

[#]Value kept fixed during the minimization procedure on least squares fitting experimental data

Table 2 Averaged values for cubic lattice parameters and mean crystallite size (actually, mean coherent length) as determined from X-ray diffraction data for this solid solution of iron oxide spinels

Sample	Lattice parameter/Å	Mean coherent length/nm
Mt	8.3625(5)	6(3)
Mt1	8.3455(8)	4(3)
Mt1Si2	8.3353(5)	3(3)

Number in parentheses is the uncertainty over the last significant digit as estimated from the standard deviation of the corresponding mean value

Mt at 298 K, it can be observed a subtle difference of intensities between lines 1 (broader and less intense) and 6, which could eventually indicate the occurrence of some $\text{Fe}^{2+}/\text{Fe}^{3+}$ character, of a residual magnetite in this sample. From corresponding spectra for samples Mt1 and Mt1Si2, this difference much less evident or is virtually absent, suggesting that only structural Fe^{3+} responds for their corresponding hyperfine structures. From these observations, any eventually existing magnetite in these samples containing mixtures of iron oxide spinels cannot be unequivocally detected, for its relatively very low amount. This assumption is in agreement with values of isomer shift from distribution profiles (Fig. 3b) and with the lattice parameters values obtained from Rietveld refinement of powder X-ray diffraction data (Table 2). Values of hyperfine field for all samples are markedly lower than those expected for a bulk maghemite or even iron oxide spinels. This is certainly due to the small sizes of particles. Spectrum for the sample Mt1Si2 is formed by a doublet of Fe^{3+} in octahedral coordination due to the iron oxide spinel dispersed on the silica matrix.

Mössbauer patterns at 80 K are shown in Fig. 3b (hyperfine parameters, Table 3). Values of isomer shift from the hyperfine field distribution are systematically higher for the Mt than for Mt1 or Mt1Si2 samples. This characteristic is a direct consequence of the higher proportion of Fe^{2+} in Mt relatively to the other two samples.

Spectra at 80 K, thus below the Verwey temperature ($T_V \approx 120$ K), reveal that for part (relative subspectral area, RA = 31 %) of sample Mt, isomer shift values vary from 0.65 mm s^{-1} to 0.82 mm s^{-1} , which may also be an evidence of some small ferrous character in the spinel phases mixture. Complementarily, subspectra due to octahedral and tetrahedral sites of maghemite would be slightly separated at this temperature, with different values of isomer shift and hyperfine field. The

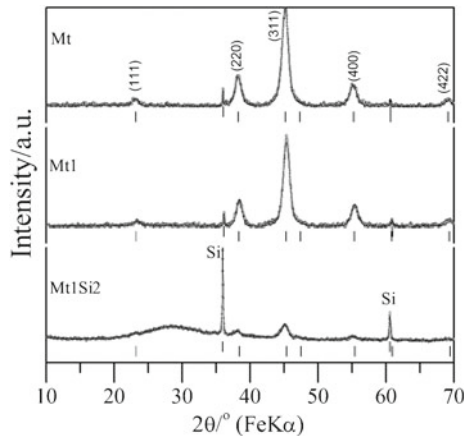
Table 3 Hyperfine parameters of the fitted Mössbauer spectra recorded at 80 K

Sample	$\delta/\text{mm s}^{-1}$	$\varepsilon/\text{mm s}^{-1}$	B_{hf}/T	RA/%
Mt	0.31	0.02	51.5	19
	0.55	0	52.2 ^a	81
Mt1	0.31	0.04	51.4	20
	0.50	-0.01	52.2 ^a	80
Mt1Si2	0.31	-0.03	51.3	22
	0.50	0.01	51.8 ^a	78

δ = isomer shift relative to αFe ; ε = quadrupole shift; Δ = quadrupole splitting; B_{hf} = hyperfine field and RA = relative subspectral area

^aHyperfine field at maximum probability of the hyperfine field distribution profile

Fig. 4 Rietveld refinement of the powder diffraction patterns of the samples Mt, Mt1 and Mt1Si2



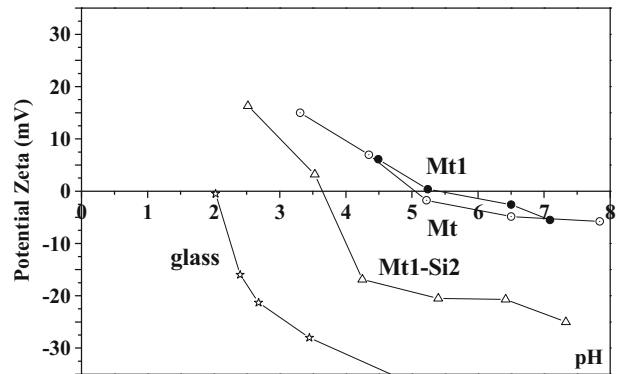
corresponding subspectrum due to this putative maghemite would present unequal relative intensities for lines 1 (more intense) and 6. This feature is indeed observed for sample Mt at 80 K. The whole spectrum may be then thought as being a multiple contribution of sites of iron oxide spinels, including a really minor occurrence of residual magnetite below the Verwey transition and of a dominant mass proportion of maghemite, presumably with some gradient in chemical stoichiometry and crystallographical structures, reflecting on the broadness of the probability profile of hyperfine field values.

Values of B_{hf} for Mt1Si2 are slightly lower than those found for samples Mt and Mt1. This is also due to the small particle sizes, as it could be confirmed by TEM images (Fig. 1) and XRD data (Table 2).

Figure 4 shows the X-ray diffraction patterns of the synthesized samples. The qualitative analysis of the XRD pattern for all samples indicated the existence of a crystallographic phase corresponding to iron oxide spinel structure, which was identified by its (111), (220), (311), (400) and (422) reflections. An amorphous contribution observed in the range of 20–35° 2θ in Mt1Si2 sample corresponds to $\text{SiO}_2 \cdot n\text{H}_2\text{O}$.

The subsequent Rietveld refinement of XRD data with Thompson-Cox-Hastings pseudo-Voigt—Axial divergence asymmetry on peak fitting gave the structural parameters summarized in Table 2 along with the mean crystallite size (actually,

Fig. 5 Zeta potential (ξ) of Mt, Mt1, Mt1Si2, and glass = hydrogel



the mean coherent length) as determined from the Scherrer equation. The average apparent crystallite size practically does not change with the treatment performed in these samples.

Fitting XRD data (patterns, Fig. 4) with Rietveld method for all samples yielded a profile residual factor, R_p , of approximately 4.7 % for each sample, indicative of good quality refined models. The pattern for sample Mt corresponds to a cubic lattice with $a = 8.3625(5)$ Å. After treatment with TMAOH the unit cell of iron oxide spinel decreases from 8.3625(5) Å in Mt sample to 8.3455(8) Å in Mt1 sample, indicating some oxidation of the Fe^{2+} in the octahedral sites of the iron oxide spinel structure, confirming what could be inferred from Mössbauer data. The unit cell of Mt1Si2 is 8.3353 Å (Table 2), suggesting a compression of the unit cell of iron oxide spinel structure. The ionic radius of the high spin Fe^{3+} on octahedral coordination is 65 pm; the corresponding value for Fe^{2+} is 78 pm. The contraction of the unit cell as it is observed for Mt1 and Mt1Si2 samples relatively to the Mt sample is due to the oxidation of Fe^{2+} to produce Fe^{3+} , with cationic vacancies in the iron oxides structures. The Fe^{2+} oxidation in the iron oxide structure should affect directly the magnetization values of these samples and consequently the amount of heat released by these nanoparticles.

To study the surface properties of the non-coated and silica-coated nanoparticles, the electrokinetics of the particles were measured and the results are presented as zeta potentials as a function of pH in Fig. 5. For comparison, the zeta potentials of silica powder are also included in this figure. The isoelectric point (IEP) of Mt was found around at pH 5.0 which is in the range of the reported value of IEP for iron oxide spinels [28]. The zeta potential is positive below the IEP and negative above the IEP. It is noted that there is different zeta potentials dependence after silica coating, which further shows that the surface properties of coated Mt sample have changed. It must be noticed that the IEP for the SiO_2 -coated particles is nearly same as that found for the pure SiO_2 particles. This confirms that SiO_2 is effectively coating the iron oxide particles, as expected.

Figure 6 shows the increase in the temperature of the samples in applied AC magnetic fields of 105 Oe and 168 Oe at 198 kHz in water and hydrogel. In the case of samples dispersed in water, the difference in the temperature of the Mt, Mt1, and Mt1-Si2 between the starting ambient temperature and that after 20 min of exposure to the magnetic field was 13, 25, and 11 °C under 168 Oe and 13, 24, and 10 °C under 105 Oe. The used magnetic field led to temperature changes for samples either in

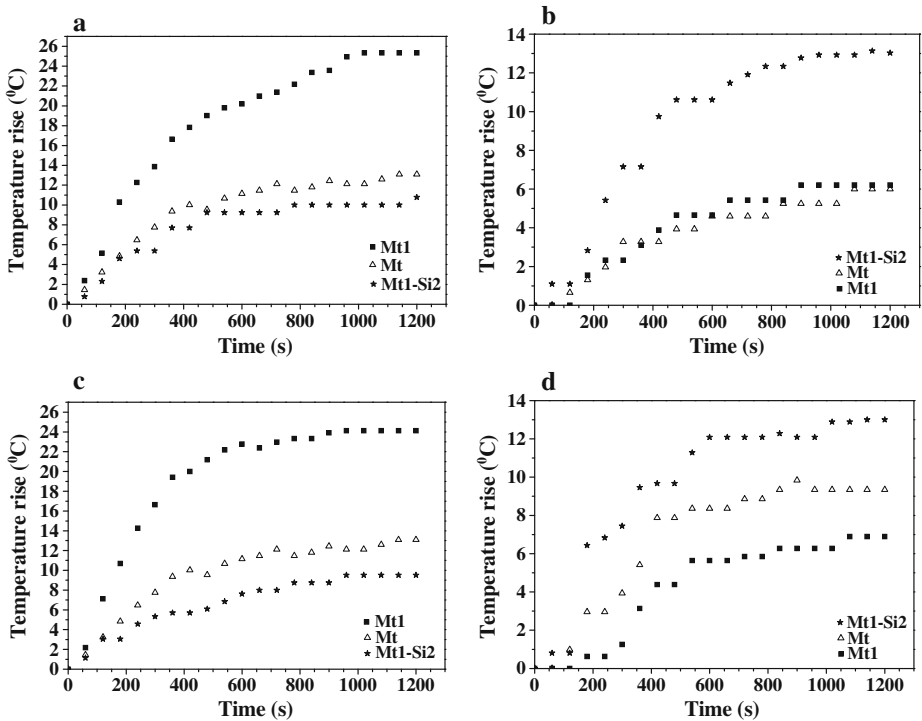


Fig. 6 Temperature–time curves of the samples: Mt, Mt1, and Mt1-Si2, in: **a** water and **b** hydro-gel at 168 Oe; and in **c** water and **d** hydrogel at 105 Oe

water (Fig. 6a and c) or in the gel (Fig. 6b and d) medium. However no difference was clearly observed for the two magnitudes of the magnetic field, which means that the magnetic field variation was not high enough to leave to temperature changes in our samples. Both samples Mt and Mt1 have similar grain size particles but the sample Mt is better dispersed. According to literature [29], Brownian rotation of an aggregate was much slower than that of single particles under an alternating magnetic field. The non-dispersed MNPs generated lower specific absorption rate (SAR) values than well-dispersed samples [30].

In the case of samples dispersed in hydrogel, the difference in the temperature of the Mt, Mt1, and Mt1-Si2 between the starting ambient temperature and that after 20 min of exposure to the magnetic field was 6, 6, and 13 °C under 168 Oe and 9, 7, and 13 °C under 105 Oe.

4 Conclusions

Iron oxide spinels nanocomposites based on iron oxide coated with silica were prepared *via* a novel simple synthesis route. The TEOS polymerization on the surface of iron oxide nanoparticles, together with TMAOH treatment, assures a well dispersed suspension in aqueous medium. Hyperthermic tests indicate that the silica-

coated composites are potentially very good materials to be used in local therapies, in oncology.

Acknowledgements Work financially supported by CNPq and FAPEMIG (Brazil; particularly grant # PPM 00419-10, APQ-04333-10, and APQ-00651-11). CAPES (Brazil) grants the Visiting Professor PVNS fellowship to JDF at UFVJM.

References

1. Andrade, A.L., Valente, M.A., Ferreira, J.M.F., Fabris, J.D.: *J. Magn. Magn. Mater.* **324**, 1753 (2012)
2. Andrade, A.L., Souza, D.M., Pereira, M.C., Fabris, J.D., Domingues, R.Z.: *Quim. Nova* **33**, 524 (2010)
3. Andrade, A.L., Souza, D.M., Pereira, M.C., Fabris, J.D., Domingues, R.Z.: *J. Nanosci. Nanotechnol.* **9**, 2081 (2009)
4. Sun, S.H., Zeng, H., Robinson, D.B., Raoux, S., Rice, P.M., Wang, S.X., Li, G.X.: *J. Am. Chem. Soc.* **126**, 273 (2004)
5. Elkins, K.E., Vedantam, T.S., Liu, J.P., Zeng, H., Sun, S.H., Ding, Y., Wang, Z.L.: *Nano Lett.* **3**, 1647 (2003)
6. Song, O., Zhang, Z.J.: *J. Am. Chem. Soc.* **126**, 6164 (2004)
7. Babincova, M., Babinec, P., Bergemann, C.: *Z. Nat. Forsch. C. J. Biosci.* **56**, 909 (2001)
8. Wang, Y.X.J., Hussain, S.M., Krestin, G.P.: *Eur. Radiol.* **11**, 2319 (2001)
9. Berry, C.C., Curtis, A.S.G.: *J. Phys. D Appl. Phys.* **36**, R198 (2003)
10. Bonnemain, B.: *J. Drug Target.* **6**, 167 (1998)
11. Laurent, S., Forge, D., Port, M., Roch, A., Robic, C., Elst, L.V., Muller, R.N.: *Chem. Rev.* **108**, 2064 (2008)
12. Mornet, S., Vasseur, S., Grasset, F., Duguet, E.: *J. Mater. Chem.* **14**, 2161 (2004)
13. Katz, E., Willner, I.: *Angew. Chem.* **43**, 6042 (2004)
14. Matsunaga, T., Okamura, Y., Tanaka, T.: *J. Mater. Chem.* **14**, 2099 (2004)
15. Pankhurst, Q.A., Connolly, J., Jones, S.K., Dobson, J.: *J. Phys. D Appl. Phys.* **36**, R167 (2003)
16. Nielsen, O.S., Horsman, M., Overgaard, J.: *Eur. J. Cancer* **37**, 1587 (2001)
17. Qu, S.C., Yang, H.B., Ren, D.W., Kan, S.H., Zou, G.T., Li, D.M., Li, M.H.: *J. Colloid Interface Sci.* **215**, 190 (1999)
18. Stober, W., Fink, A., Bohn, E.: *J. Colloid Interface Sci.* **26**, 62 (1968)
19. Andrade, A.L., Souza, D.M., Pereira, M.C., Fabris, J.D., Domingues, R.Z.: *Cerâmica* **55**, 420 (2009)
20. Hyon, S.H., Cha, W.I., Ikada, Y.: *Polym. Bull.* **22**, 119 (1989)
21. Andrade, A.L., Fabris, J.D., Ardisson, J.D., Valente, M.A., Ferreira, J.M.F.: *J. Nanomater.* **2012**, 1 (2012)
22. Schwertmann, U., Cornell, R.M.: In: Schwertmann, U., Cornell, R.M. (eds.) *Iron Oxides in the Laboratory: Preparation and Characterization* (1991)
23. Ouasri, A., Rhandour, A., Dhamelin court, M.C., Dhamelin court, P., Mazzah, A.: *Spectrochim. Acta, Part A: Mol. Biomol. Spectrosc.* **58**, 2779 (2002)
24. Li, Y.S., Church, J.S., Woodhead, A.L., Moussa, F.: *Spectrochim. Acta, Part A: Mol. Biomol. Spectrosc.* **76**, 484 (2010)
25. Barrado, E., Prieto, F., Medina, J., Lopez, F.A.: *J. Alloys Compd.* **335**, 203 (2002)
26. de Vidales, J.L.M., Lopez-Delgado, A., Vila, E., Lopez, F.A.: *J. Alloys Compd.* **287**, 276 (1999)
27. Ma, M., Zhang, Y., Yu, W., Shen, H.Y., Zhang, H.Q., Gu, N.: *Colloids Surf., A Physicochem. Eng. Asp.* **212**, 219 (2003)
28. Erdemoglu, M., Sarikaya, M.: *J. Colloid Interface Sci.* **300**, 795 (2006)
29. Erne, B.H., Butter, K., Kuipers, B.W.M., Vroege, G.J.: *Langmuir* **19**, 8218 (2003)
30. Wang, X.M., Gu, H.C., Yang, Z.Q.: *J. Magn. Magn. Mater.* **293**, 334 (2005)